

## METABOLISM

# Metabolic recycling of ammonia via glutamate dehydrogenase supports breast cancer biomass

Jessica B. Spinelli,<sup>1,2</sup> Haejin Yoon,<sup>1</sup> Alison E. Ringel,<sup>1</sup> Sarah Jeanfavre,<sup>2</sup> Clary B. Clish,<sup>2</sup> Marcia C. Haigis<sup>1\*</sup>

Ammonia is a ubiquitous by-product of cellular metabolism; however, the biological consequences of ammonia production are not fully understood, especially in cancer. We found that ammonia is not merely a toxic waste product but is recycled into central amino acid metabolism to maximize nitrogen utilization. In our experiments, human breast cancer cells primarily assimilated ammonia through reductive amination catalyzed by glutamate dehydrogenase (GDH); secondary reactions enabled other amino acids, such as proline and aspartate, to directly acquire this nitrogen. Metabolic recycling of ammonia accelerated proliferation of breast cancer. In mice, ammonia accumulated in the tumor microenvironment and was used directly to generate amino acids through GDH activity. These data show that ammonia is not only a secreted waste product but also a fundamental nitrogen source that can support tumor biomass.

Increased nutrient consumption can supply carbon, nitrogen, oxygen, and sulfur to accommodate the extensive bioenergetic, biosynthetic, and prosurvival requirements of rapidly proliferating cells (1–3). As a consequence, such cells generate an excess of metabolic waste products, which are cleared in mammals through the excretory system. However, in the tumor microenvironment, metabolic waste products such as lactate and ammonia accumulate (4, 5). Although lactate is well studied in cancer, little is known about the mechanisms by which cancer cells manage increased amounts of ammonia (NH<sub>3</sub>) generated by glutamine and asparagine catabolism, de novo cysteine synthesis through the transsulfuration pathway, and salvage nucleotide metabolism (6). Ammonia has been considered a toxic by-product that must be exported from cells and is subsequently cleared through urea cycle activity in the liver (7–9).

Glutamine has been called a “nitrogen reservoir” for cancer cells because of its anabolic role in nucleotide synthesis (6, 10). However, the role of glutamine as a nitrogen reservoir is contradicted in catabolic glutamine metabolism, because nitrogen is liberated as the by-product ammonia (11). The fate of ammonia in the metabolism of proliferating cells and tumors remains unclear. We hypothesized that ammonia might be reassimilated into central metabolism to maximize the efficiency of nitrogen utilization. In this study, we sought to clarify the role of ammonia as either a toxic waste product or a biosynthetic metabolite (Fig. 1A).

Mammals have three enzymes that can overcome the thermodynamic hurdles of ammonia

assimilation: (i) carbamoyl phosphate synthetase I (CPS1), the adenosine triphosphate (ATP)-dependent, rate-limiting step of the urea cycle; (ii) glutamate dehydrogenase (GDH), a NADPH (reduced nicotinamide adenine dinucleotide phosphate)-dependent enzyme that catalyzes the reductive amination of  $\alpha$ -ketoglutarate; and (iii) glutamine synthetase (GS), which catalyzes the ATP-dependent amination of glutamate to generate glutamine (12, 13) (fig. S1A). Analysis of transcriptomic data from The Cancer Genome Atlas for the ammonia-assimilating enzymes in healthy and cancerous tissues revealed that expression of GS and GDH mRNA is significantly increased across many cancer subtypes, whereas CPS1 mRNA is increased only in the colon (Fig. 1B). Among healthy tissues, GS and GDH are ubiquitously expressed and CPS1 is expressed only in the liver (fig. S1B). Breast cancers display increased expression of both GS and GDH. Specifically, estrogen receptor-positive (ER<sup>+</sup>) breast cancers have increased expression of GS and GDH relative to that in other subtypes (14). Therefore, we used ER<sup>+</sup> breast cancer as a representative model to probe for ammonia assimilation.

To investigate the fate of glutamine-derived ammonia, we performed a metabolic tracing analysis with hydrophilic interaction liquid chromatography tandem mass spectrometry (HILIC-MS) and assessed the fate of [<sup>15</sup>N]amide-glutamine, which liberates [<sup>15</sup>N]NH<sub>3</sub> through glutaminase activity (15). To identify the metabolic derivatives of [<sup>15</sup>N]amide-glutamine in an unbiased manner, we developed a method to screen the nitrogen metabolome, which contained 211 <sup>15</sup>N-isotopologs (table S1). The majority of the nitrogen metabolome did not acquire <sup>15</sup>N labeling; of 211 <sup>15</sup>N-isotopologs, only 33 metabolites were labeled (fig. S2). Consistent with previous studies, [<sup>15</sup>N]amide-glutamine was incorporated into asparagine and nucleotides (10) (Fig. 1C and fig. S3A). We also

identified <sup>15</sup>N-isotopologs of proline, aspartate, branched-chain amino acids (BCAAs), and glutamate, which have no previous biosynthetic connection to the amide nitrogen on glutamine (Fig. 1C and fig. S3B). The labeled nitrogen was liberated as ammonia before production of these metabolites, which suggests that an ammonia-recycling pathway may synthesize the other glutamine derivatives detected.

To test whether ammonia released during glutaminolysis was necessary for production of these unanticipated amide-nitrogen glutamine derivatives, we treated cells with the glutaminase inhibitor bis-2-(5-phenylacetamido-1,3,4-thiadiazol-2-yl)ethyl sulfide (BPTES), which at 1  $\mu$ M is not cytotoxic or cytostatic in T47D and MCF7 human breast cancer cell lines (16) (fig. S4, A to C). BPTES treatment significantly decreased <sup>15</sup>N-isotopologs of glutamate, proline, and aspartate, whereas metabolites involved in direct glutamine metabolism, such as nucleotides and asparagine, remained labeled (Fig. 1D and fig. S4D). Addition of ammonia to BPTES-treated cells restored metabolites depleted by glutaminase inhibition, demonstrating the specific contribution of ammonia (fig. S4E). This is consistent with findings that ammonia partially rescues proliferative defects in glutamine-deprived breast cancer cells (17).

We examined the potential mechanisms underlying assimilation of ammonia liberated during glutaminolysis. Because [<sup>15</sup>N]amide-glutamine did not elicit any isotopes of four urea cycle intermediates (ornithine, citrulline, argininosuccinate, and arginine), we ruled out the activity of CPS1 as a mechanism for ammonia assimilation (fig. S2). Instead, our data indicated that GDH was the primary point of ammonia assimilation because glutamate is upstream of proline, aspartate, glutamine, and BCAA synthesis. However, the Michaelis-Menten constant ( $K_m$ ) of GDH for ammonia is high (approximately 9 mM) and GDH reportedly favors oxidative deamination over reductive amination in cancer cells (18–21). By contrast, GDH-catalyzed reductive amination is prevalent in the liver, where there is a sufficient concentration of ammonia to enable catalysis in this direction (22). We wondered whether increased concentrations of ammonia in the tumor microenvironment might also permit GDH-catalyzed reductive amination.

To determine whether GDH assimilates ammonia generated by glutamine catabolism, we used short hairpin RNA (shRNA) to deplete cells of GDH, cultured them with [<sup>15</sup>N]amide-glutamine, and then subjected them to nitrogen metabolome scanning (fig. S4F). MCF7 and T47D cell lines express both GDH1 and GDH2 isoforms, and shRNAs targeted both isoforms (fig. S4G). The abundance of <sup>15</sup>N-isotopologs of glutamate and downstream metabolites (proline, aspartate) was significantly decreased in cells depleted of GDH (Fig. 1E). Urea cycle intermediates (citrulline, argininosuccinate) remained unlabeled in cells lacking GDH, underscoring the lack of CPS1-mediated ammonia assimilation in breast

<sup>1</sup>Department of Cell Biology, Harvard Medical School, Boston, MA 02115, USA. <sup>2</sup>Broad Institute of MIT and Harvard, Cambridge, MA 02142, USA.

\*Corresponding author. Email: marcia\_haigis@hms.harvard.edu

cancer cells (Fig. 1E). Reexpression of shRNA-insensitive GDH1 rescued labeling onto glutamate and downstream metabolites (fig. S5).

Next, we used a liquid chromatography–mass spectrometry method for the detection of [ $^{15}\text{N}$ ]NH $_3$

from [ $^{15}\text{N}$ ]amide-glutamine (23) to measure the amount of [ $^{15}\text{N}$ ]NH $_3$  generated after 8 hours of treatment with [ $^{15}\text{N}$ ]amide-glutamine. In MCF7 and T47D cells, we found that only 3.5% of the total ammonia pool derived from glutaminolysis

(fig. S6, A to C). Because ~2% of the glutamate pool acquired this label in a glutaminase-dependent manner (fig. S3B), we hypothesized that ammonia recycling from glutaminolysis is highly efficient. We quantified the efficiency of ammonia

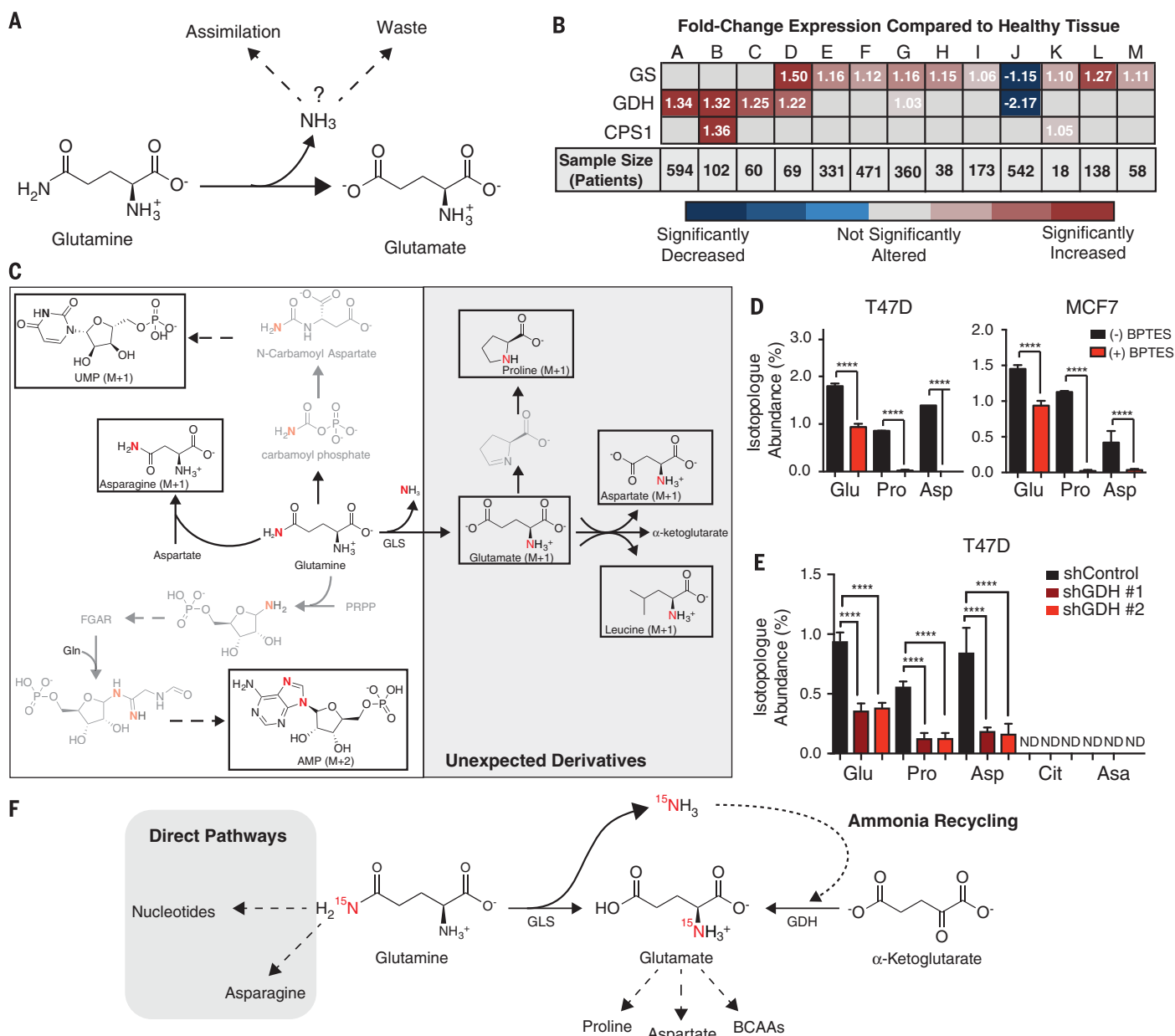


**Fig. 1. Glutamine-derived ammonia is recycled. (A)** Schematic of fates of ammonia in cancer. **(B)** mRNA expression of ammonia-assimilating enzymes from The Cancer Genome Atlas in cancerous versus normal tissue. GS (glutamine synthetase), GDH1 (glutamate dehydrogenase), and CPS1 (carbamoyl phosphate synthetase 1) RNA levels were assessed using Oncomine.org; values are the mean of fold change (cancer/normal, where normal = 1.00) measured across the sample size shown at the bottom. A, ovarian serous cystadenocarcinoma; B, colon adenocarcinoma; C, rectal adenocarcinoma; D, lobular and ductal breast carcinoma; E, lung adenocarcinoma; F, squamous lung cell carcinoma; G, endometrial adenocarcinoma; H, bladder urothelial carcinoma; I, gastric adenocarcinoma; J, glioblastoma; K, pancreatic adenocarcinoma; L, hepatocellular carcinoma; M, cutaneous

melanoma. **(C)** Schematic of  $^{15}\text{N}$ -isotopologs after treatment with [ $^{15}\text{N}$ ]amide-glutamine. UMP, uridine monophosphate; PRPP, phosphoribosyl pyrophosphate; FGAR, 5'-phosphoribosyl-N-formylglycineamide; AMP, adenosine monophosphate. **(D)** Isotopolog abundance of unexpected [ $^{15}\text{N}$ ]amide-glutamine derivatives  $\pm 1 \mu\text{M}$  BPTES in T47D and MCF7 cell lines. Values are means  $\pm$  SEM;  $n = 4$  per condition. **(E)** Isotope abundance of [ $^{15}\text{N}$ ]amide-glutamine-derived metabolites in control cells and cells depleted of GDH (shGDH #1 and shGDH #2). Glu, glutamate M+1; Pro, proline M+1; Asp, aspartate M+1; Cit, citrulline M+1; Asa, argininosuccinate M+1; ND,  $^{15}\text{N}$ -isotopolog not detected. Values are means  $\pm$  SEM;  $n = 4$  per condition. **(F)** Schematic of ammonia recycling. GLS, glutaminase. \*\*\*\* $P < 0.0001$  (two-tailed  $t$  test for all comparisons).

recycling from glutamine catabolism by incubating MCF7 cells with [ $^{15}\text{N}_2$ - $^{13}\text{C}_5$ ]glutamine. Glutaminolysis generated [ $^{15}\text{N}$ - $^{13}\text{C}_5$ ]glutamate (glutamate M+6), and ammonia recycling was measured by detection of [ $^{15}\text{N}$ ]glutamate (glutamate M+1) (fig. S6D). We calculated the ratio

of the total amount of glutamate (glutamate M+6 and glutamate M+1) to glutamate directly generated in glutaminolysis (glutamate M+6) (fig. S6E). In total, 1.57 molecules of glutamate were generated from a single reaction of glutaminolysis, indicating a 57% efficiency of

ammonia recycling (fig. S6F). Because both processes are mitochondrial, localization may support this high efficiency (24). GDH is a bi-directional enzyme, so we also tested whether the catalytic activity of oxidative deamination or reductive amination was prevalent. In GDH-depleted cells, ammonia recycling (glutamate M+1) was decreased, but  $\alpha$ -ketoglutarate (M+5) was unchanged, suggesting a net activity of reductive amination in this system (fig. S6, G and H). In sum, these data indicate that ammonia derived from glutaminolysis is recycled by reductive amination catalyzed by GDH to support the synthesis of glutamate and downstream metabolites (Fig. 1F).

Because numerous reactions other than glutaminolysis generate ammonia, we investigated whether free ammonia could be assimilated into metabolic pathways. To optimize  $\text{NH}_4\text{Cl}$  for tracing studies, we investigated whether exposure to increased concentrations of  $\text{NH}_4\text{Cl}$  was toxic to tumor cells. Physiological concentrations of ammonia in plasma are 0 to 50  $\mu\text{M}$  in healthy human adults, 50 to 150  $\mu\text{M}$  in newborns, and up to 1.0 mM in patients with hyperammonemia (25). Supraphysiological concentrations of ammonia are toxic to neurons and are sometimes assumed to be toxic to tumor cells (7, 26, 27). However,  $\text{NH}_4\text{Cl}$  was not toxic to tumor cells, even at concentrations that were toxic to primary human astrocytes (Fig. 2A and fig. S7A). Previous reports have shown that high concentrations of ammonia induce autophagy in tumor cells (5). In MCF7 and T47D cell lines, light chain 3 II (LC3II) lipidation was not induced until 10 mM ammonia was added to media—a concentration exceeding levels of ammonia reported in the tumor microenvironment (fig. S7B). Moreover, ammonia concentrations of 0 to 10 mM did not alter uptake of glucose or glutamine, nor basal respiration (fig. S7, C to E). Expression of the ammonia-assimilating enzymes GS, GDH, and CPS1 was not affected by increasing ammonia concentration (fig. S7, F to I), nor did 10 mM ammonia alter the pH of the culture media (fig. S7J). These data indicate that supraphysiological concentrations of ammonia did not induce toxicity or metabolic stress in breast cancer cells.

We also examined ammonia uptake by cells. When breast cancer cells were cultured in low concentrations of ammonia (0 to 1.0 mM), we observed a net output of ammonia, which reverted to net uptake as the extracellular concentration of  $\text{NH}_4\text{Cl}$  increased above 1 mM (fig. S7K). At approximately 1.0 mM  $\text{NH}_4\text{Cl}$ , ammonia was taken up from the medium, such that ammonia entry may be regulated by diffusion. In agreement with this result, the characterized mechanism of ammonium ( $\text{NH}_4^+$ ) import and export is through facilitated diffusion with rhesus glycoproteins (RhC and RhG) (28). Also, ammonia can diffuse across the plasma membrane.

We performed steady-state and tracing experiments in the presence of 0.75 mM  $\text{NH}_4\text{Cl}$  because it is the inflection point of ammonia uptake and secretion and represents a low concentration of ammonia that is relevant to the

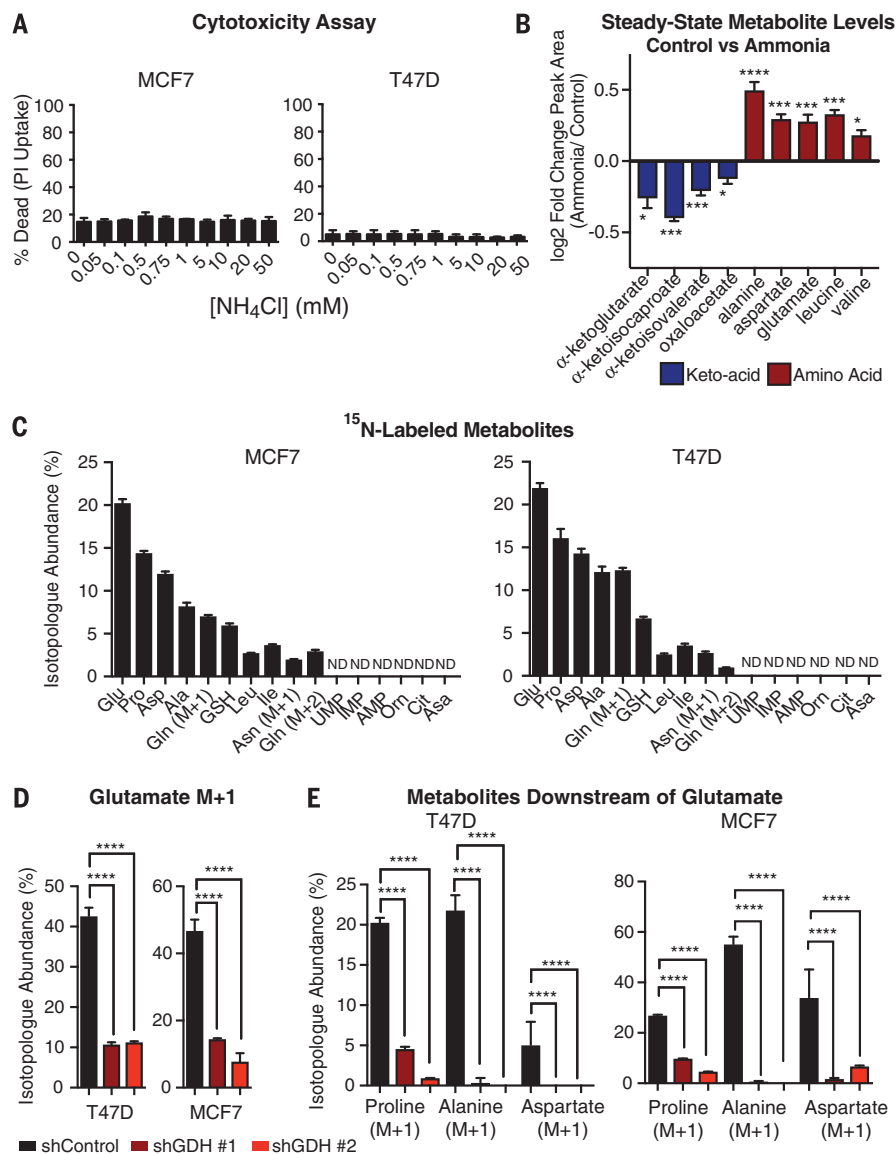


**Fig. 2. Ammonia is assimilated by GDH to generate amino acids.** (A) Propidium iodide (PI) staining of cells treated with a dose of  $\text{NH}_4\text{Cl}$  for 48 hours. Values are means  $\pm$  SEM from a representative experiment of three replicates;  $n = 3$ . (B) Abundance of keto- and amino acids involved in transaminase reactions in T47D cells treated with 0.75 mM  $\text{NH}_4\text{Cl}$ . Values are means  $\pm$  SEM from a representative experiment of two replicates;  $n = 4$ . (C) Abundance of  $^{15}\text{N}$ -isotopologs in MCF7 and T47D cells after 8 hours of treatment with 0.75 mM [ $^{15}\text{N}$ ]  $\text{NH}_4\text{Cl}$ . (M+1) and (M+2) indicate labeling with one or two nitrogens, respectively. Values are scaled to account for total intracellular ammonia and represent means  $\pm$  SEM;  $n = 4$ . (D) Isotopolog abundance of glutamate (M+1) in MCF7 and T47D cells treated for 8 hours with 0.75 mM [ $^{15}\text{N}$ ]  $\text{NH}_4\text{Cl}$  in control and GDH-depleted cells. Values are scaled to account for total intracellular ammonia and represent means  $\pm$  SEM;  $n = 4$ . (E) Abundance of  $^{15}\text{N}$ -isotopologs for metabolites downstream of glutamate treated for 8 hours with 0.75 mM [ $^{15}\text{N}$ ]  $\text{NH}_4\text{Cl}$  in control and GDH-depleted cells. Values are scaled to account for total intracellular ammonia and represent means  $\pm$  SEM;  $n = 4$ . \* $P < 0.05$ , \*\*\* $P < 0.001$ , \*\*\*\* $P < 0.0001$  (two-tailed  $t$  test for all comparisons).

tumor microenvironment. We used MetaboAnalyst 3.0 to perform an unbiased pathway analysis on the steady-state metabolites from cells cultured with or without ammonia (fig. S8A). The most significantly altered pathway was glutamate, aspartate, and alanine metabolism. Exposure to  $\text{NH}_4\text{Cl}$  elicited a signature of increased transaminase activity, whereby the abundance of ketoacids decreased and that of amino acids derived from them increased (Fig. 2B). Although amounts of nonessential amino acids increased, the abundance of other amino acids remained unchanged by ammonia, indicating that ammonia did not affect universal amino acid metabolism (fig. S8B). Nor did ammonia alter the abundance of metabolites from the urea cycle and nucleotides (fig. S8, C and D).

MCF7 and T47D cells were treated with 0.75 mM [ $^{15}\text{N}$ ] $\text{NH}_4\text{Cl}$  and scanned for  $^{15}\text{N}$ -isotopologs (fig. S9). Isotopolog abundances were scaled to represent total ammonia pools, because treatment with 0.75 mM enriched ~35% of the intracellular ammonia pool (table S2). Consistent with tracing performed with glutamine-derived ammonia, we detected  $^{15}\text{N}$  labeling of glutamate and downstream metabolites, such as proline and aspartate (Fig. 2C). Upon tracing with low levels of ammonia, a striking 20% of the glutamate pool was labeled, implying an important role for ammonia assimilation in glutamate metabolism in cancer, as glutamate levels are high (millimolar) (11). Tracing with high levels of ammonia that have been reported in the tumor microenvironment (3 mM) also elicited the same signature of ammonia assimilation (fig. S10A).

Consistent with steady-state data, all of the amino acids labeled were generated through glutamate-dependent transaminase reactions, except proline and glutathione, which were made in direct synthetic pathways from glutamate (fig. S10B). Other nitrogen-containing metabolites (particularly urea cycle intermediates) and essential amino acids were not labeled by ammonia (fig. S9). Furthermore, even though ammonia generated  $^{15}\text{N}$ -isotopologs of glutamine, we detected no  $^{15}\text{N}$ -isotopologs of any nucleotides, which is distinct from ammonia metabolism in serine-threonine kinase II (STKII)-low tumors (29). We speculate that because labeled glutamine is generated in the mitochondria, this pool may not access the cytoplasm where de novo nucleotide synthesis occurs, rendering nucleotides unlabeled.

A time course of [ $^{15}\text{N}$ ] $\text{NH}_4\text{Cl}$  tracing revealed that ammonia was rapidly converted into glutamate, the first metabolite to reach steady state (fig. S10, C to F). Thus, ammonia appears to be primarily assimilated to generate glutamate, and other labeled metabolites are produced in secondary reactions. We therefore investigated which metabolic derivatives of ammonia required GDH activity. In cells depleted of GDH, [ $^{15}\text{N}$ ] $\text{NH}_4\text{Cl}$  labeling of glutamate was diminished, as was labeling of metabolites downstream of glutamate (Fig. 2, D and E). Indeed, this labeling was rescued

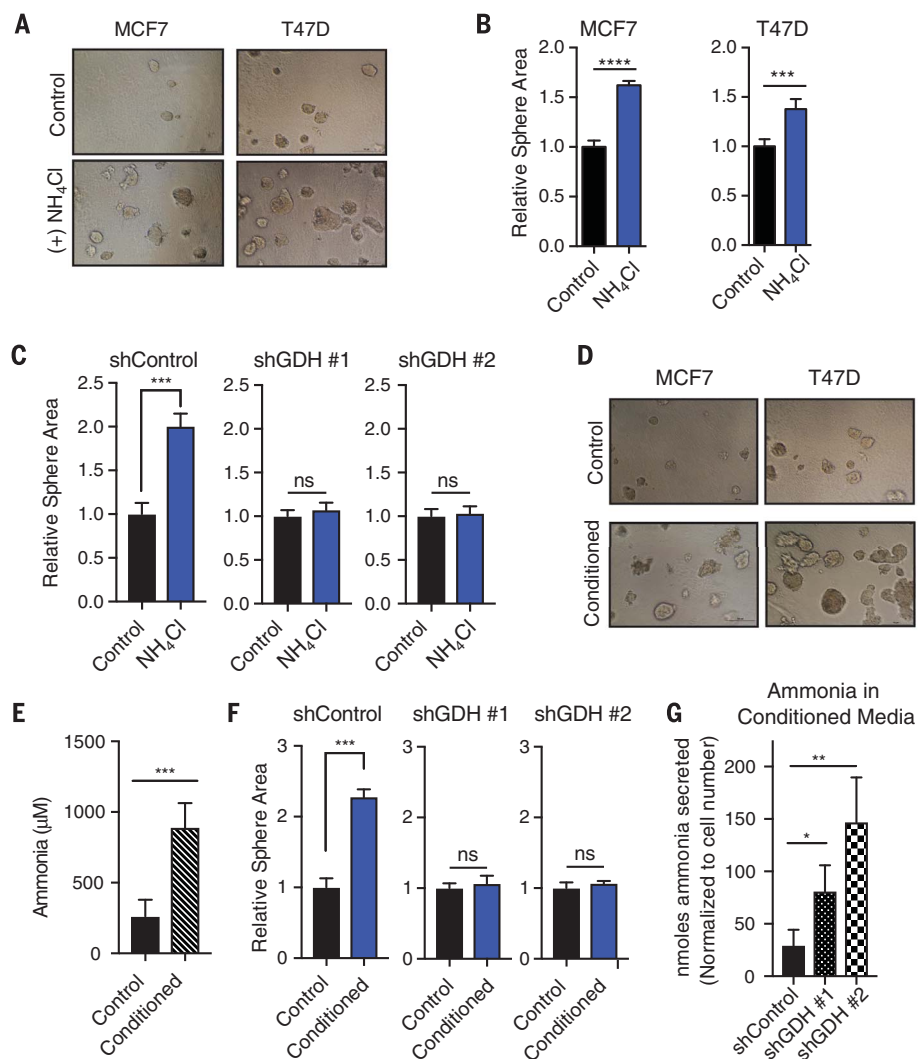


**Fig. 3. Ammonia stimulates breast cancer growth and proliferation.** (A) Representative images of 3D culture models of MCF7 and T47D cells treated with 0.5 mM  $\text{NH}_4\text{Cl}$  compared to control conditions. (B) Quantification of average sphere area of 100 to 200 spheres per well in 3D culture models of MCF7 and T47D cells treated with ammonia and control conditions for 7 days. Values are mean areas  $\pm$  SEM from a representative experiment of five replicates;  $n = 4$ . (C) Quantification of average sphere area of 200 to 250 spheres per well in 3D culture models of MCF7 cells harboring stable shRNA-mediated knockdown of GDH or control hairpin. Cells were treated for 8 days. Values are mean areas  $\pm$  SEM from a representative experiment of three replicates;  $n = 4$ . (D) Representative images of MCF7 and T47D cells in control conditions (medium changed daily) and conditioned media (medium changed every 72 hours). Cells were treated for 8 days. (E) Ammonia measurement in conditioned media compared to control after 8 days. (F) Quantification of average sphere area of 200 to 250 spheres per well in 3D culture models of MCF7 control cells or cells depleted of GDH. Cells were treated in control or conditioned media for 8 days. Values are mean areas  $\pm$  SEM from a representative experiment of three replicates;  $n = 4$ . (G) Nanomoles of ammonia secreted per cell after 72 hours in control cells or cells depleted of GDH. Values are means  $\pm$  SEM;  $n = 3$ . \* $P < 0.05$ , \*\* $P < 0.01$ , \*\*\* $P < 0.001$ , \*\*\*\* $P < 0.0001$  (two-tailed  $t$  test for all comparisons); ns, not significant.

when shRNA-insensitive GDH1 was overexpressed (fig. S10, G and H). We did not observe adaptation through the ammonia-assimilating enzymes GS or CPS1 in cells lacking GDH. In both T47D and MCF7 cells, glutamine and asparagine labeling did not change in cells depleted of GDH (fig. S11). Metabolites of the urea cycle were unlabeled in

cells depleted of GDH, indicating that adaptive reprogramming of ammonia assimilation into the urea cycle is not important in cultured breast cancer cells (fig. S9). Our data reveal a general mechanism by which free ammonia in the tumor microenvironment can be harnessed for biosynthetic pathways.

Ammonia assimilation in yeast has a fundamental role in supporting growth and proliferation (30, 31). Because ammonia was not toxic to tumor cells (Fig. 2A), we tested whether ammonia might facilitate growth and proliferation of breast cancer cells. As in yeast, addition of  $\text{NH}_4\text{Cl}$  to cell culture media increased proliferation in breast cancer cell lines (fig. S12, A and B). The culture medium was changed daily to minimize ammonia accumulation, which we measured to be approximately 0.3 mM per day from glutamine degradation and cellular metabolism (fig. S12, C and F). Moreover, in 3D culture, in which cells are suspended in matrigel and form “spheres” for growth, addition of ammonia to media stimulated sphere growth and cell proliferation (Fig. 3, A and B, and fig. S12G). However, proliferation of primary human fibroblasts was not changed when ammonia was added to culture media (fig. S13A). Using  $^{15}\text{N}$  tracing, we found that fibroblasts centrally assimilated ammonia to generate glutamine (fig. S13B), in line with their high expression of glutamine synthetase (32). Moreover,  $^{15}\text{N}$  amide-glutamine tracing revealed that fibroblasts did not recycle glutamine-derived ammonia to generate glutamate, aspartate, or proline (fig. S13C). Thus, we hypothesized that ammonia assimilation to generate glutamate through GDH may be important for its role in increased proliferation observed in breast cancer cells. Indeed, depletion of GDH prevented the accelerated growth of breast cancer cells treated with ammonia (Fig. 3C). Interestingly, the glutamate derivatives proline, aspartate, and glutathione are associated with proliferation and tumorigenesis (33–37).

To assess the effect of tumor-generated ammonia on growth and proliferation, we compared the ability of cancer cells to grow in 3D cultures in which the medium was changed either daily or every 3 days, allowing ammonia to accumulate. The latter procedure provided a growth advantage for breast cancer cells, which correlated with ammonia accumulation in the media (Fig. 3, D and E). Therefore, we tested whether ammonia recycling through GDH was a critical aspect that influenced proliferation. Cells depleted of GDH had no growth defect when the culture medium was changed daily, but the growth advantage when medium was changed after 3 days was abrogated (Fig. 3F and fig. S14, A to C). Furthermore, cells depleted of GDH secreted more ammonia into the medium, consistent with impairment of ammonia recycling (Fig. 3G). In addition, treatment of MCF7 cells in 3D culture with high ammonia concentrations (3 mM  $\text{NH}_4\text{Cl}$ ) also stimulated proliferation (fig. S14D).

To examine the physiological relevance of ammonia in the tumor microenvironment in vivo, we measured concentrations of ammonia that accumulated in the interstitial fluids of  $\text{ER}^+$  xenograft tumors.  $\text{ER}^+$  xenografts accumulated 0.8 to 3 mM ammonia in the interstitial fluids of the tumor microenvironment, whereas plasma ammonia concentrations were approximately 300  $\mu\text{M}$

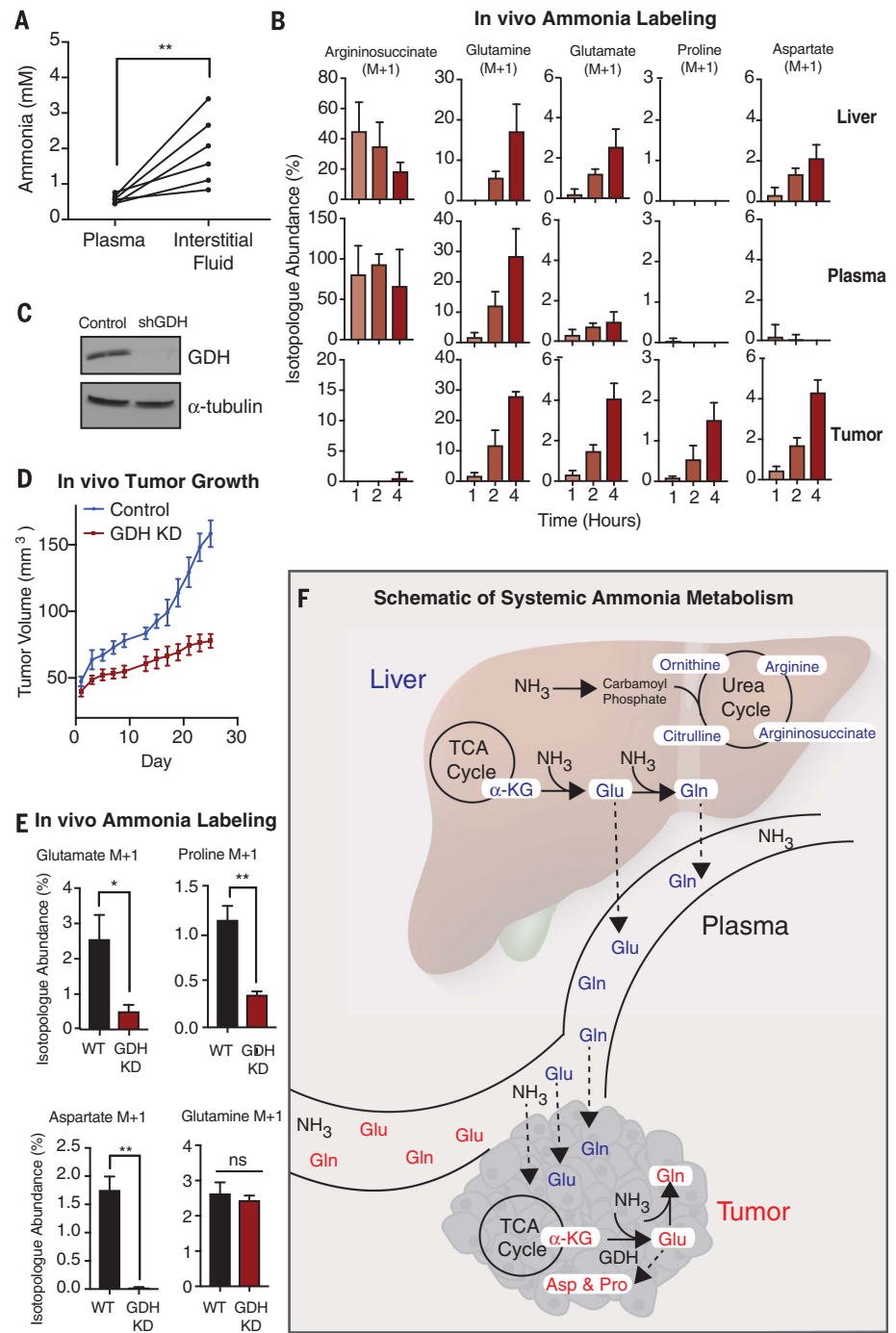


**Fig. 4. Contributions of systemic and tumor-autonomous ammonia metabolism to amino acid synthesis.** (A) Measurement of ammonia in the interstitial fluids of the tumor microenvironment (TME) compared to plasma isolated from  $\text{ER}^+$  breast cancer xenograft models. Lines connect values of ammonia in the plasma to that in the interstitial fluid of the TME. (B) Isotope abundance of  $^{15}\text{N}$ -isotopologs isolated from the liver, plasma, and tumor of mice intraperitoneally injected with a bolus (9.0 mmol/kg) of  $^{15}\text{N}$   $\text{NH}_4\text{Cl}$ . Tissues were harvested 1, 2, or 4 hours after injection. Values are means  $\pm$  SEM;  $n = 4$ .  $^{15}\text{N}$ -isotopologs were corrected for natural abundance of tissues harvested from a control mouse treated with  $\text{NH}_4\text{Cl}$  (9.0 mmol/kg) for 4 hours. (C) Western blot of GDH knockdown in T47D xenograft tumors. (D) In vivo tumor growth of T47D control and GDH-depleted (GDH KD) xenograft models ( $n = 15$  mice per group). Values are mean tumor volumes  $\pm$  SEM. (E) In vivo tracing of  $^{15}\text{N}$   $\text{NH}_4\text{Cl}$  in T47D control and GDH-depleted xenograft models. Values are mean isotopologue abundances  $\pm$  SEM;  $n = 4$ . (F) Schematic of systemic and tumor-autonomous ammonia metabolism. TCA, tricarboxylic acid;  $\alpha$ -KG,  $\alpha$ -ketoglutarate. \* $P < 0.05$ , \*\* $P < 0.01$  (two-tailed  $t$  test for all comparisons).

(Fig. 4A). This range of concentrations did not induce autophagy and was shown to accelerate growth and proliferation in vitro. Plasma ammonia concentrations in mice harboring tumors were not different from those in control mice (fig. S15A).

We tested whether accumulated ammonia in the tumor microenvironment was assimilated into metabolic pathways in vivo. Mice harboring subcutaneous T47D breast tumors were intraperitoneally injected with [ $^{15}\text{N}$ ]NH $_4$ Cl, and the tumor, liver, and plasma were assessed for  $^{15}\text{N}$ -isotopologs over the next 1 to 4 hours (fig. S15B). The liver and tumor used distinct metabolic pathways for ammonia assimilation (Fig. 4B and figs. S16 and S17A). In the liver, ammonia was sequestered into the urea cycle, leading to labeling of ornithine, citrulline, argininosuccinate, and arginine (fig. S16). Although these labeled intermediates of the urea cycle were also detected in the plasma, they were undetectable in the tumor, indicating that these breast tumors did not engage the urea cycle for ammonia assimilation in vivo (Fig. 4B and fig. S16). Proline and aspartate, which were identified in vitro as metabolic derivatives of ammonia, were also labeled in the tumor in vivo. The metabolic pathways enabling proline and aspartate labeling were likely from tumor-autonomous metabolism, as labeled proline and aspartate were not detected in the plasma (Fig. 4B).

We also observed labeling of glutamine and glutamate in the tumor. Because labeled glutamine and glutamate were also found in the liver and plasma, it is not clear whether these  $^{15}\text{N}$ -isotopologs were generated tumor-autonomously. Furthermore, the kinetics of glutamine labeling in the tumor implied that a subset of the labeled glutamine pool in the tumor may be taken up from the plasma (Fig. 4B).

To distinguish systemic contributions of ammonia metabolism from tumor-autonomous metabolic pathways, we traced [ $^{15}\text{N}$ ]NH $_4$ Cl and [ $^{15}\text{N}$ ]amide-glutamine in tumors ex vivo (fig. S17, B to D). With [ $^{15}\text{N}$ ]NH $_4$ Cl, labeling of glutamate, aspartate, proline, and glutamine was recapitulated. Consistent with in vivo studies, the urea cycle intermediates, nucleotides, and other nitrogen-abundant metabolites were not labeled. These data underscore a fundamental role of ammonia for amino acid synthesis, particularly glutamate, aspartate, and proline in vivo.

Consistent with in vitro experiments, tumors treated with [ $^{15}\text{N}$ ]amide-glutamine generated labeled glutamate as well as the downstream metabolites proline and aspartate, suggesting that glutamine-derived ammonia may be recycled in solid tumors (fig. S18A). In contrast to free [ $^{15}\text{N}$ ]NH $_4$ Cl, which did not label metabolites of the urea cycle in cells in vivo or in solid tumors ex vivo, [ $^{15}\text{N}$ ]amide-glutamine, when added to the tumors ex vivo, elicited labeling of the urea cycle intermediate citrulline (fig. S17D). Thus, an alternative pathway that does not require ammonia may exist that connects the amide nitrogen on glutamine to citrulline production ex vivo.

We next generated a GDH-depleted xenograft model to further investigate the mechanism of ammonia assimilation in vivo (Fig. 4C). Tumor-specific depletion of GDH significantly decreased tumor growth in vivo, consistent with our findings that GDH-depleted cells grow slower in conditioned media and are insensitive to ammonia-induced growth in vitro (Fig. 4D and fig. S18A). Because GDH-catalyzed ammonia assimilation mediates growth and proliferation in vitro, we used intraperitoneal injection of [ $^{15}\text{N}$ ]NH $_4$ Cl in control and GDH-depleted xenograft models to test whether GDH also assimilates ammonia in vivo. Glutamate, aspartate, and proline labeling were significantly decreased in GDH-depleted tumors relative to control tumors (Fig. 4E). GDH depletion did not abrogate glutamine labeling, underscoring the specificity of GDH for ammonia assimilation to generate glutamate and the downstream metabolites proline and aspartate.

To further validate that GDH-mediated ammonia assimilation is tumor-autonomous, we traced ammonia ex vivo in control and GDH-depleted tumors. GDH depletion significantly decreased glutamate, aspartate, and proline labeling (fig. S18B). Taken together, these data show that tumor biomass is supported by both tumor-autonomous metabolism of ammonia and systemic assimilation, especially for glutamate-derived amino acids (Fig. 4F).

Ammonia accumulates in the tumor microenvironment because tumors are poorly vascularized, making this a unique niche for ammonia metabolism in the human body. Because ammonia transport is mediated by diffusion, elevated ammonia in the microenvironment leads to its accumulation inside of tumor cells (fig. S18C). Therefore, the ability to reassimilate this ammonia into metabolic pathways is critical in this context. In contrast, the liver reassimilates ammonia to generate urea, which is a sink for excess nitrogen and is excreted as metabolic waste to protect against toxicity associated with systemic ammonia accumulation. Tumor cells strictly recycle this nitrogen to generate amino acids downstream of glutamate and do not engage the urea cycle.

Our findings show that ammonia is an important nitrogen source for breast cancer metabolism. Ammonia is not simply a metabolic waste product, and it can be recycled to support the high demand for amino acid synthesis in rapidly proliferating cells. Although ammonia is sometimes considered a toxin, it stimulated growth and proliferation in breast cancer cells. This stimulatory effect appears to be mediated by GDH-catalyzed ammonia assimilation. Furthermore, ammonia accumulated in the tumor microenvironment and was used by cancer cells for amino acid synthesis in vivo. These biosynthetic pathways are supported in both systemic and tumor-autonomous metabolism. Thus, metabolic recycling of ammonia provides an important source of nitrogen for breast cancer biomass.

## REFERENCES AND NOTES

- N. N. Pavlova, C. B. Thompson, *Cell Metab.* **23**, 27–47 (2016).
- S. Vyas, E. Zaganjor, M. C. Haigis, *Cell* **166**, 555–566 (2016).
- J. L. Colloff et al., *Cell Metab.* **23**, 867–880 (2016).
- M. G. Vander Heiden, L. C. Cantley, C. B. Thompson, *Science* **324**, 1029–1033 (2009).
- C. H. Eng, K. Yu, J. Lucas, E. White, R. T. Abraham, *Sci. Signal.* **3**, ra31 (2010).
- B. J. Altman, Z. E. Stine, C. V. Dang, *Nat. Rev. Cancer* **16**, 619–634 (2016).
- M. Kappler et al., *Clin. Oral Investig.* **21**, 211–224 (2017).
- E. B. Tapper, Z. G. Jiang, V. R. Patwardhan, *Mayo Clin. Proc.* **90**, 646–658 (2015).
- R. J. DeBerardinis, T. Cheng, *Oncogene* **29**, 313–324 (2010).
- S. Tardito et al., *Nat. Cell Biol.* **17**, 1556–1568 (2015).
- R. J. DeBerardinis et al., *Proc. Natl. Acad. Sci. U.S.A.* **104**, 19345–19350 (2007).
- M. M. Adeva, G. Souto, N. Blanco, C. Donapetry, *Metabolism* **61**, 1495–1511 (2012).
- S. M. Morris Jr., *Annu. Rev. Nutr.* **22**, 87–105 (2002).
- S. Tyanova et al., *Nat. Commun.* **7**, 10259 (2016).
- A. L. S. Lee, D. Roberts, R. E. Gerszten, C. B. Clish, Targeted metabolomics. *Curr. Protoc. Mol. Biol.* 30.32.31–30.32.24 (2012).
- M. M. Robinson et al., *Biochem. J.* **406**, 407–414 (2007).
- M. Meng, S. Chen, T. Lao, D. Liang, N. Sang, *Cell Cycle* **9**, 3921–3932 (2010).
- F. Frigerio, M. Casimir, S. Carobbio, P. Maechler, *Biochim. Biophys. Acta* **1777**, 965–972 (2008).
- J. R. Treberg, M. E. Brosnan, M. Watford, J. T. Brosnan, *Adv. Enzyme Regul.* **50**, 34–43 (2010).
- M. E. Brosnan, J. T. Brosnan, *Am. J. Clin. Nutr.* **90**, 857S–861S (2009).
- J. Adam et al., *Cell Rep.* **3**, 1440–1448 (2013).
- I. Zaganas et al., *Metab. Brain Dis.* **28**, 127–131 (2013).
- J. B. Spinelli, L. P. Kelley, M. C. Haigis, *Sci. Rep.* **7**, 10304 (2017).
- B. Masola, T. M. Devlin, *Amino Acids* **9**, 363–374 (1995).
- S. Dasarthy et al., *Metab. Brain Dis.* **32**, 529–538 (2017).
- O. Braissant, V. A. McClain, C. Cudalbu, *J. Inher. Metab. Dis.* **36**, 595–612 (2013).
- P. Hillmann, M. Köse, K. Söhl, C. E. Müller, *Toxicol. Appl. Pharmacol.* **227**, 36–47 (2008).
- F. Gruswitz et al., *Proc. Natl. Acad. Sci. U.S.A.* **107**, 9638–9643 (2010).
- J. Kim et al., *Nature* **546**, 168–172 (2017).
- V. M. Boer, C. A. Crutchfield, P. H. Bradley, D. Botstein, J. D. Rabinowitz, *Mol. Biol. Cell* **21**, 198–211 (2010).
- S. Laxman, B. M. Sutter, L. Shi, B. P. Tu, *Sci. Signal.* **7**, ra120 (2014).
- T. Vermeulen et al., *Arch. Biochem. Biophys.* **478**, 96–102 (2008).
- J. M. Phang, W. Liu, C. N. Hancock, J. W. Fischer, *Curr. Opin. Clin. Nutr. Metab. Care* **18**, 71–77 (2015).
- N. Sahu et al., *Cell Metab.* **24**, 753–761 (2016).
- L. Jin et al., *Cancer Cell* **27**, 257–270 (2015).
- K. Birsoy et al., *Cell* **162**, 540–551 (2015).
- L. B. Sullivan et al., *Cell* **162**, 552–563 (2015).

## ACKNOWLEDGMENTS

The authors acknowledge all members of the Haigis lab for insightful discussions. Supported by the Ludwig Center at Harvard, Glenn Foundation for Medical Research, and NIH grant R01CA213062 (M.C.H.) and by NSF Graduate Research Fellowship Program grant DGE1144152 (J.B.S.). M.C.H. and J.B.S. are inventors on patent application HMV- 27560 submitted by Harvard Medical School that covers ammonia utilization in cancer.

## SUPPLEMENTARY MATERIALS

www.sciencemag.org/content/358/6365/941/suppl/DC1  
Materials and Methods  
Figs. S1 to S18  
Tables S1 and S2  
References (38–42)

7 February 2017; accepted 29 September 2017  
Published online 12 October 2017  
10.1126/science.aam9305

## Metabolic recycling of ammonia via glutamate dehydrogenase supports breast cancer biomass

Jessica B. Spinelli, Haejin Yoon, Alison E. Ringel, Sarah Jeanfavre, Clary B. Clish and Marcia C. Haigis

*Science* **358** (6365), 941-946.

DOI: 10.1126/science.aam9305 originally published online October 12, 2017

### Cancer cells put ammonia back to work

Ammonia, often considered a metabolic waste product, can be recycled to build new amino acids. Rapidly proliferating cells produce extracellular nitrogen. Spinelli *et al.* used metabolic tracing of  $^{15}\text{N}$  to follow the fate of extracellular ammonia and its incorporation into more than 200 components of the nitrogen metabolome (see the Perspective by Dang). Accumulation of ammonia enabled glutamate dehydrogenase to function in reductive amination, which allowed incorporation of nitrogen from ammonia back into amino acids. Experiments in mice also showed incorporation of ammonia into glutamate, aspartate, and proline.

*Science*, this issue p. 941; see also p. 862

#### ARTICLE TOOLS

<http://science.sciencemag.org/content/358/6365/941>

#### SUPPLEMENTARY MATERIALS

<http://science.sciencemag.org/content/suppl/2017/10/11/science.aam9305.DC1>

#### RELATED CONTENT

<http://science.sciencemag.org/content/sci/358/6365/862.full>  
<http://stm.sciencemag.org/content/scitransmed/7/274/274ra17.full>  
<http://stm.sciencemag.org/content/scitransmed/5/198/198ra108.full>  
<http://stm.sciencemag.org/content/scitransmed/2/31/31ra34.full>  
<http://stm.sciencemag.org/content/scitransmed/2/31/31ed1.full>  
<http://stke.sciencemag.org/content/sigtrans/10/510/eaao6604.full>

#### REFERENCES

This article cites 41 articles, 8 of which you can access for free  
<http://science.sciencemag.org/content/358/6365/941#BIBL>

#### PERMISSIONS

<http://www.sciencemag.org/help/reprints-and-permissions>

Use of this article is subject to the [Terms of Service](#)